

Observation of Trapped Anomalous Cosmic Rays with MIDORI Satellite

H. Miyasaka¹, T. Kohno¹, I. Yamagiwa¹, H. Kato¹, C. Kato², T. Goka³ and H. Matsumoto³

¹*Institute of Physical and Chemical Research(RIKEN), Saitama 351-0198, Japan*

²*Department of Physics, Shinshu University, Nagano 390-8621, Japan*

³*National Space Development Agency of Japan, Ibaraki 305-0047, Japan*

Abstract

The Heavy Ion Telescope (HIT) on board the Japanese satellite MIDORI (its name before launch was ADEOS) has measured the heavy ions at 800km altitude during nine months between October 1996 and June 1997. We have analyzed the geomagnetically trapped oxygen near $L=2$. These particles were considered to be originating from singly ionized interplanetary anomalous cosmic rays (ACRs) which are trapped after being stripped their electrons in the Earth's upper atmosphere. Average energy spectra, pitch angle distribution and their temporal variations were investigated at $R=1.31$. It was found that the pitch angle distributions were nearly isotropic outside the loss cone at $60^\circ < \alpha_1 < 120^\circ$ except a dip existing around $\alpha_1=90^\circ$. The particle intensity was stable in time during the observation period when the solar activity was low. The spatial distribution of the omnidirectional intensity at $R < 1.31$ is also presented.

1 Introduction:

The satellite MIDORI was launched by NASDA (National Agency of Space Development of Japan) for the observations of the Earth. The satellite is on a sun-synchronous orbit with an altitude of ~ 800 km and inclination of 98.6° . A heavy ion telescope, HIT (Kohno et al., 1997), on board this satellite have observed the geomagnetically trapped particles. HIT has a geometric factor of ~ 25 cm² and covers an energy range of 18-53 MeV/nuc for oxygen. The trapped particles were also observed previously by COSMOS (e.g. Grigorov et al., 1991) and SAMPEX (e.g. Cummings et al., 1993). From the earlier analyses, these particles were considered to be originating from singly ionized interplanetary anomalous cosmic rays (ACRs) which are trapped after being stripped their electrons in the Earth's upper atmosphere. Their analyses confirmed the expectation by Blake and Friesen (1977) that the ACRs can be trapped in the geomagnetic field.

In this brief report, we analyze the intensity of the trapped ACR oxygens by using data observed at ~ 800 km during nine months between the beginning of October 1996 and the end of June 1997.

2 Analysis of the trapped ACRs:

We picked up the trapped ACR events simply by analyzing data in the region of $1.5 < L < 2.5$, $B < 27000$ nT and $\epsilon Q < 1.0$, where ϵ and Q are respectively the adiabaticity parameter and particle's charge. The product ϵQ represents an upper limit of charged particle to be trapped. Since we do not measure charge state Q directory, ϵQ is given by the Earth's dipole moment of 7.84×10^{15} Tm³, as

$$\epsilon Q = 5.18 \times 10^{-5} A [E(E + 1863)]^{1/2} L^2 \quad (1)$$

where E is particle's kinetic energy in MeV per nucleon, A the atomic mass number. We used the International Geomagnetic Reference Field (IGRF) 1995 model for the local magnetic field.

To evaluate the trapped particle intensity, we followed the method of Selesnik et al. (1995) which were adopted to the SAMPEX observation (Selesnick et al., 1995, 1995 ; Looper et al., 1996). With notations used in Selesnik et al., 1995, the intensity of the trapped ACRs can be described by a function, $j_1(E, a1, L, t)$, of L value, time t and the pitch angle α_1 which is transformed from the observed pitch angle α , as

$$\sin^2 \alpha_1 = \frac{B_0 L^3}{B R_1^3} \left(4 - \frac{3R_1}{L} \right)^{\frac{1}{2}} \sin^2 \alpha \quad (2)$$

where R_1 is the dipole equivalent radius in unit of the Earth's radius B and B_0 are the magnetic field magnitudes at the observation point and on the equator with same L -shell, respectively. We set $R_1=1.31$ corresponding to the highest point where MIDORI observed the trapped ACRs. We further assume that j_1 can be expressed, as

$$j_1(E, \alpha_1, L, t) \equiv U(E, L)V(\alpha_1)W(t) \quad (3)$$

where $U(E, L)$ represents the time average energy spectrum perpendicular to magnetic field on each L -shell, $V(\alpha_1)$ is the pitch angle distribution normalized to unity at $\alpha_1 = 90^\circ$ and $W(t)$ represents the temporal variation. The functions on the right hand side of equation (3) can be calculated, as

$$U = \frac{\sum_{\alpha_1, t} N}{\sum_{\alpha_1, t} V W \bar{H}}, \quad V = \frac{\sum_{E, L, t} N}{\sum_{E, L, t} U W \bar{H}}, \quad W = \frac{\sum_{E, L, \alpha_1} N}{\sum_{E, L, \alpha_1} U V \bar{H}} \quad (4)$$

where $N(E, L, \alpha_1, t)$ is the observed count of ACRs in each of E -, L -, α_1 - and t -bins and $H(E, L, \alpha_1, t)$ is the response function of HIT which we evaluated from the Monte Carlo simulations taking accounts of the geometry of HIT and the exposure of HIT to ACRs on the orbit of MIDORI.

Figure 1 shows the energy spectra (U) of oxygen calculated for seven L values indicated at the top of each panel between $L=1.57$ and $L=2.33$. This figure shows the fluxes at $\alpha_1 = 90^\circ$. The arrow in each panel indicates the cutoff energy estimated from the local western cutoff rigidity for the singly charged oxygen. Figure 2 shows the pitch angle distribution (V) (top panel) and the observed distribution of α_1 (bottom panel) which was transformed from the observed α by equation (2). MIDORI observed the trapped ACRs only from the Southern Hemisphere and two peaks on both sides of $\alpha_1 = 90^\circ$ correspond to the up- and down-streams. The asymmetry of these two peaks in the bottom panel is due to less response to up-stream of HIT, which HIT always viewing opposite to the Earth. The top panel of Figure 3 shows the temporal variation of intensity

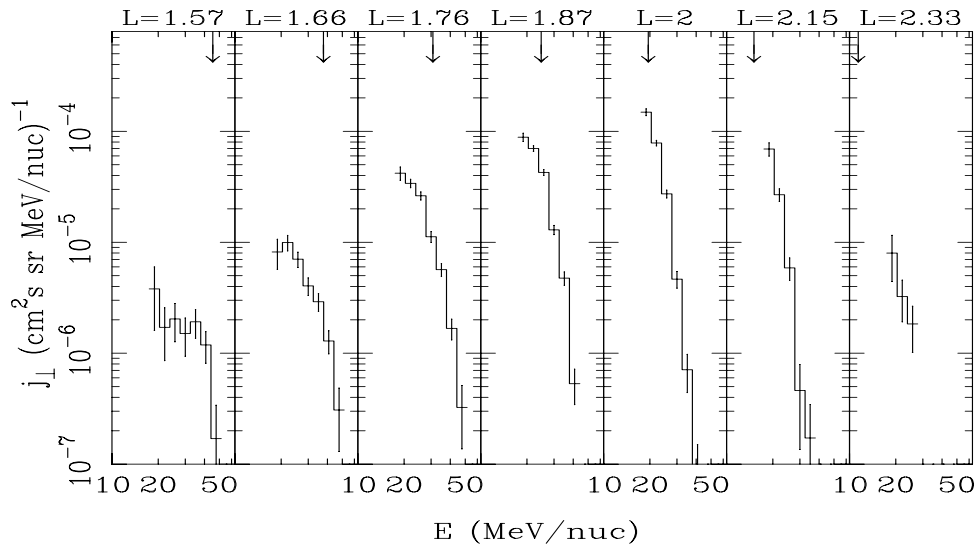


Figure 1: Average energy spectra (U) of the trapped ACR oxygen calculated at $R=1.31$. Each of seven panels shows spectrum for L -value indicated at the top. The energy ranges from 18 to 53 MeV/nuc. The arrow in each panel indicates the cutoff energy estimated from the local western cutoff rigidity for the singly charged oxygen. Errors are deduced from counts in each bin.

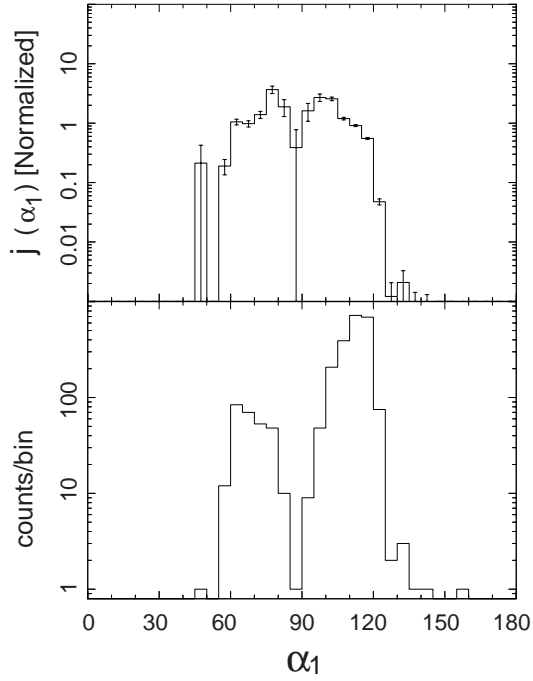


Figure 2: The pitch angle distribution (V) normalized to unity at $\alpha_1=90^\circ$ (top) and the observed distribution of α_1 (bottom) of the trapped ACR oxygen. Errors are deduced from counts in each bin.

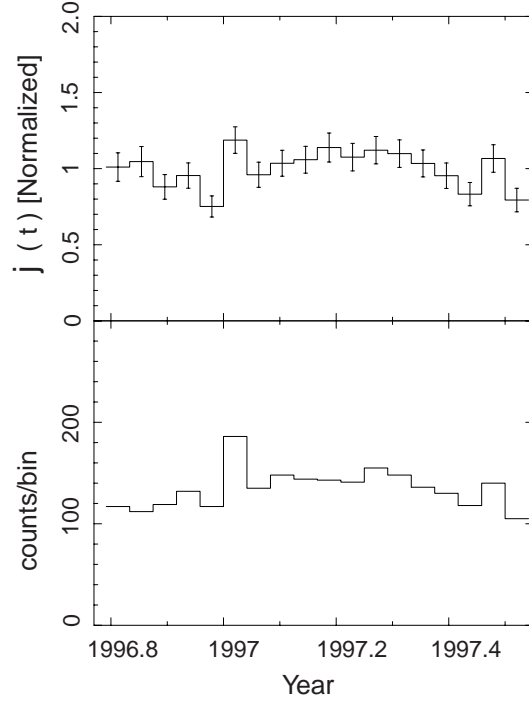


Figure 3: Temporal variation of intensity (W) normalized to the average intensity over the total observation period (top) and the variation of the observed count of the trapped ACR oxygen (bottom). Errors are deduced from counts in each bin.

(W) normalized to the average intensity over the total observation period, while the bottom panel shows the variation of the observed count of the trapped ACR oxygen. All errors in Figures 1 to 3 are deduced from counts in each bin.

3 Summary and discussion:

The energy spectra of the trapped ACR oxygen in Figure 1 have peaks around the cutoff energy and steeply decrease in higher energy regions. The spectra are flatter in the lower energy regions. The maximum flux is observed around the cutoff energy at $L=2.0$. The pitch angle distribution of the trapped oxygen shows the loss-cone at $\alpha_1 < 60^\circ$ and $\alpha_1 > 120^\circ$ (see Figure 2). The intensity outside the loss-cone is roughly isotropic except a dip existing around $\alpha_1 = 90^\circ$. The statistic is not enough in Figure 2, but quite similar structure is also reported from the observation by SAMPEX (Selesnick et al., 1997). During the observation period of MIDORI, the intensity of the trapped ACRs was stable in time (see Figure 3). This seems to be consistent with the low solar activity during the observation period of MIDORI.

Figure 4 shows a counter map of the omnidirectional intensity I_{omni} of the trapped ACRs observed at south tip of the SAA region. The intensity is represented in gray scale in unit of $\log(\text{oxygens}/\text{cm}^2/\text{s})$. The intensity at $R=1.31$ on the right edge of this figure was deduced from the energy spectra and the pitch angle distribution by

$$I_{omni} = \int \int U(E, L) V(\alpha) dE d\alpha \quad (5)$$

where integrating region were $E > 18 \text{ MeV/n}$ and $60^\circ < \alpha < 120^\circ$. The intensity at $R < 1.31$ was calculated by using equation (2) under assumption that the trapped particle does not travel across the L -shell. From

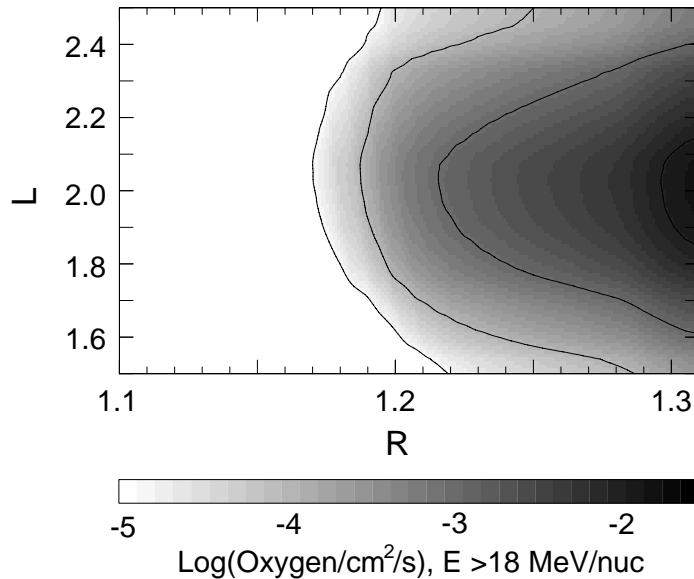


Figure 4: Omnidirectional intensity map of trapped oxygen in gray scale at the region of $1.5 < L < 2.5$ and $1.1 < R < 1.31$. The right side of edge ($R=1.31$) are the intensity which have estimated at section 2. The solid lines show the counter of intensity at -5.0, -4.0, -3.0 and -2.0 in $\text{Log}(\text{Oxygen}/\text{cm}^2/\text{s})$.

this figure, we could find the atmospheric interaction region existing around $R=1.17\sim 1.19$. The intensity at $R=1.30$ seems to be lower than the result reported from the observation by SAMPEX (Selesnick et al., 1997), even if we take account of the fact that the energy region covered by HIT is slightly narrower than that by SAMPEX (the low energy threshold of HIT is 18 MeV/n, while it is 15 MeV/n in SAMPEX).

The geographical distribution of the trapped ACRs (Kohno et al., 1997) together with the distribution in Figure 4 may allow us to investigate the three dimensional structure of the trapped region. For such analysis, however, we need to compare our result with others at different altitudes, such as results from SAMPEX and COSMOS. We also need to develop another models as well.

Acknowledgments

The HIT was calibrated by heavy ion beam from RIKEN Ring Cyclotron. We would like to acknowledge the support and efforts of the staff of the Riken accelerator facility.

References

- Blake, J.B. & Friesen, M.L., 1977, Proc. 15th ICRC (Plovdiv, 1977), 2, 341
 Cummings, J.R., Cummings, A.C., Mewaldt, R.A., Selesnick, R.S., Stone, E.C. & T.T. von Rosenvinge, 1993, Geophys. Res. Lett., 20, 2003
 Grigorov, N.L., Kondratyeva, M.A., Panasyuk, M.I., Tretyakova, C.A., Adams Jr, J.H., Blake, J.B., Schulz, M., Mewaldt, R.A. & Tylka, A.J., 1991, Geophys. Res. Lett., 18, 1959
 Kohno, T., Yamagiwa, I., Miyasaka, H., Goka, T., Matsumoto, H., 1997, Proc. 25th ICRC (Darban, 1997), 2, 317
 Looper, M.D., Blake, J.B., Klecker, B., & Hovestadt, D., 1996, J. Geophys. Res. 101, 24,747
 Selesnick, R.S., Cummings, A.C., Cummings, J.R., Mewaldt, R.A., Stone, E.C., & T.T. von Rosenvinge, 1995, J. Geophys. Res. 100, 9503
 Selesnick, R.S., Leske, R.A., Mewaldt, R.A., & Cummings, J.R., 1997, Proc. 25th ICRC (Darban, 1997), 2, 305